Modulated Periodic Stokes Waves in Deep Water

M. J. Ablowitz
Department of Applied Mathematics, University of Colorado, Boulder, Colorado 80309

J. Hammack and D. Henderson
Department of Mathematics, Pennsylvania State University, University Park, Pennsylvania 16802

C. M. Schober
Department of Mathematics and Statistics, Old Dominion University, Norfolk, Virginia 23529
(Received 3 August 1999)

Modulated deep-water 1D Stokes waves are considered experimentally and theoretically. Wave trains are modulated in a controlled fashion and their evolution is recorded. Data from repeated laboratory experiments are reproducible near the wave maker, but diverge away from the wave maker. Numerical integration of a perturbed nonlinear Schrödinger equation and an associated linear spectral problem indicate that under suitable conditions modulated periodic Stokes waves evolve chaotically. Sensitive spectral evolution in the neighborhood of homoclinic manifolds of the unperturbed nonlinear Schrödinger equation is found.

PACS numbers: 47.35.+i, 05.45.Yv, 47.11.+j, 47.20.Ky

In 1847 Stokes obtained approximate nonlinear periodic solutions of the water wave equations [1]. In 1926 Levi-Civita proved that the series obtained by Stokes' method coverged [2]. Subsequently, Benjamin and Feir showed that the Stokes wave was unstable in deep water [3]. The result can be stated as follows: if the Stokes wave is slowly modulated in sufficiently deep water, the wave is, in fact, unstable. The modulation is described, to leading order, by the nonlinear Schrödinger equation (NLS).

The NLS is a completely integrable Hamiltonian system and possesses a large class of quasiperiodic solutions [4]. On the basis of NLS theory, one generically expects to have near recurrence of initial states [5]. However, water wave dynamics are described by NLS only to leading order in an asymptotic expansion (based on small amplitudes and slowly modulated wave trains). We find that perturbations to NLS in the water waves context can cause serious nonlinear instabilities and chaos to develop.

Earlier work on computational chaos in the NLS equation demonstrated that small perturbations to the NLS, even roundoff errors, can generate chaotic solutions for initial data in sensitive regions, i.e., near homoclinic manifolds [6]. With symmetric data, $u(-x,t) = u(x,t)$, the mechanism for chaotic behavior involves random crossings of the critical level sets of the constants of motion or "homoclinic crossings" [6,7]. With nonsymmetric data, solutions of perturbed NLS do not generically exhibit homoclinic crossings; rather transition states occur nearby the homoclinic manifolds. The solutions are characterized by random "homoclinic transitions" between left and right going waves [8]. The homoclinic transitions lead to temporally irregular, chaoticlike transitions in the waveform between six different physical states.

In the present study we examine whether chaotic evolutions can be observed in the water wave approximation to NLS [see Eq. (3)]. Our main findings are (i) consistent evidence in the laboratory and numerical experiments of nonrepeatability and chaos; (ii) a nonlinear spectral analysis of the data shows that the spectrum evolves into sensitive homoclinic regimes where homoclinic transitions occur. The phenomenon of nonreproducibility of water wave experiments bears strong similarities to discrete problems where computational chaos arises despite the fact that the perturbations to the NLS equation are entirely different.

Laboratory experiments.—The experiments were conducted in a wave tank 14.3 m in length by 25.4 cm in width and 20 cm in depth. At this depth it is sufficient to use the deep water limit. A computer-controlled wave maker at one end of the tank generates waves with programmed position and velocity corresponding to the surface displacement and its derivative of either a soliton or a modulated periodic wave train. Five gauges, which average over the width of the tank, measured the surface displacement of the water. Gauge 0 is fixed at 40 cm downstream from the wave maker and its data are analyzed to ensure that the initial surface displacement near the wave maker is reproducible. Gauges 1–4 were mounted 40 cm apart on a movable carriage that spans the length of the tank. Two types of time series are obtained from these gauges: a fixed frame series obtained as the wave propagates past the fixed gauges and a moving frame series obtained by setting the carriage in motion (at the linear group speed) after transient effects die out.

In the temporal measurements we compare time series obtained from different experiments with identical initial conditions. These measurements are graphed against each other to produce a "phase plane" diagnostic for reproducibility. If the results of the two experiments are identical the graph will be the 45° line. In particular, the time series from gauge 0 near the wave maker produces a 45°

line with a very slight width, indicating a (1–2)% noise level. This indicates what should be expected from time series showing the wave field evolution.

Envelope solitons.—The control experiment is performed with the soliton solution of NLS since theoretically it should evolve reproducibly (see below). The wave maker was programmed to oscillate as $\eta_s(t) = a\sin(\omega_0 t)\mathrm{sech}(\frac{a\omega_0 t}{\sqrt{2}})$, where $\omega_0 = 20.94$ rad/sec, $a = 0.2$ cm, $k_0 = 0.44$ rad/cm, $\omega'(k_0) = 24.4$ cm/sec (group velocity), $g = 980$ cm/sec^2, and $T = 71.9$ dyn/cm (surface tension).

To determine if the soliton experiment is reproducible the experiment was run every 15 min over a $2\frac{1}{2}$ h period. Time series are obtained at gauge 4 when the carriage was 800 cm downstream of the wave maker. Figure 1a graphs the water surface displacements measured in the first and last experiments against each other. There was a slight phase shift between the two data sets. Shifting each data point in one of the data sets the same amount (0.009 21 sec) produces the nearly perfect 45° line (Fig. 1a). There is also some amplitude decay due to damping. This indicates that we obtain a reproducible experiment when the initial conditions are solitons and supports the notion that, for envelope solitons for the time scales under consideration, the unperturbed NLS equation [(3) for $\epsilon = 0$] yields a satisfactory description of the long time dynamics.

Modulated periodic wave trains.—For modulated wave trains the position of the wave maker is programmed to be $\eta_p(t) = a\sin(\omega_0 t)(1 + \delta_E \sin\omega_p t)$, where $a = 0.5$ cm, $\omega_p = 1.047$ rad/sec, $\delta_E = 0.1$, the values ω_0, g, k_0, T are the same as in the soliton case, and the corresponding unperturbed periodic wavelength of the modulation is $L = 147$ cm. For this initial data, phase plane plots show that the wave is reproducible near the wave maker. However, as the wave travels down the tank we obtain Lissajous-type figures (see, e.g., Fig. 1b) indicating that a phase shift develops between the waves of the two experiments which is a function of time and cannot be removed. Unlike the soliton, the two time series start to diverge, indicating the experiment is irreproducible.

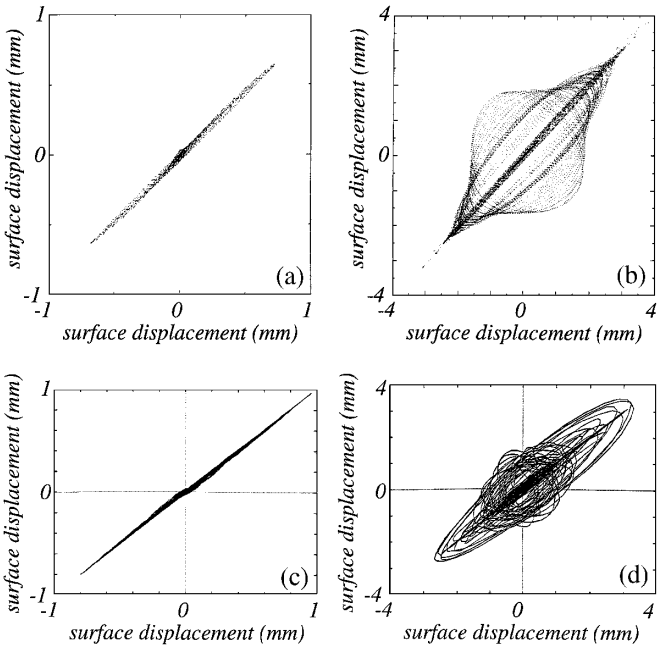

FIG. 1. Phase plane plots for (a) experimental soliton data, (b) experimental modulated wave train data, (c) numerical soliton data, and (d) numerical modulated wave train data.

Spatial data associated with modulated periodic wave trains were also obtained yielding a different perspective of the evolution. The spatial envelope is reconstructed by concatenating 40 sets of data for each of the four gauges. In the 40 experiments the initial location of the carriage differs by 1 cm successively for each experiment. At 21.3 sec after the wave maker was started, the carriage begins traversing the tank at the group velocity of the underlying wave train. The result is 160 time series of the water surface spaced 1 cm apart which are used to reconstruct the spatial profile of the water surface, 160 cm long. Our ability to measure a spatial envelope by conducting 40 experiments requires the experiments to be reproducible.

In tracking the spatial envelope of the modulated wave train, data taken near the wave maker are used to provide a benchmark for the level of noise. In reconstructing the envelope by concatenating the data sets, the "blips" in the data are miniscule at gauge 0 near the wave maker. At $t = 15$ sec, the waveform is somewhat close to the wave maker and the blips in the data are not significant (Fig. 2a). Farther down the tank additional crests start to form. The blips become significant and no longer represent a simple nonsmoothness in the wave profile. By 40 sec, the periodicity of the underlying wave train is lost (Fig. 2b). The degeneration of the spatial coherence of the wave field indicates that the experiments are not reproducible. This experimental irreproducibility and the theory presented below are evidence that modulated Stokes wave trains evolve chaotically for certain parameter regimes.

Analytical background.—The equations governing the surface waves are given by $\nabla^2\phi = 0$, for $z \le \eta$, $\phi_z \to 0$ as $z \to -\infty$, where $\phi(x, z, t)$, $\eta(x, t)$ are the velocity potential and free surface displacement, respectively, and, by the boundary conditions on the free surface $z = \eta(x, t)$,

$$\eta_t + \eta_x\phi_x = \phi_z; \qquad \phi_t + g\eta + \frac{1}{2}(\nabla\phi)^2 = 0. \tag{1}$$

In the small amplitude approximation, the velocity potential is expanded about $z = 0$. For slowly modulated waves one assumes the ansatz

$$\phi = \epsilon(Ae^{i\vartheta + |k|z} + *) + \epsilon^2(\bar{\phi} + A_2 e^{2(i\vartheta + |k|z)} + *)\ldots,$$
$$\eta = \epsilon(Be^{i\vartheta} + *) + \epsilon^2(\bar{\eta} + B_2 e^{2i\vartheta} + *) + \ldots, \tag{2}$$

where $\theta = kx - \omega t$, * denotes complex conjugate, and the deep water dispersion relation is used: $\omega^2 = g|k|$ with

$k_0 = 0.44$ rad/cm (neither damping or surface tension is taken into account in the theory). The variables $A, \bar{\phi}, A_2$ are functions of $X = \epsilon x, Z = \epsilon z, T = \epsilon t$, and $B, \bar{\eta}, B_2$ are functions of X and T only. ϵ is dimensionless and is a measure of small amplitude and balances slow modulation; $\epsilon = ka$, where a is the size of the initial surface displacement. Substituting the above ansatz into the expanded form of the free surface Eq. (1) leads to the following perturbed NLS equation on $z = 0$ [9]:

$$2i\omega\left(A_T + \frac{\omega}{2k}A_X\right) - \epsilon\left[\left(\frac{\omega}{2k}\right)^2 A_{XX} + 4k^4|A|^2A\right] = \epsilon^2\left(\frac{i\omega^2}{8k^3}A_{XXX} + 2k^3iA^2A_X^* - 12k^3i|A|^2A_X + 2\omega k\bar{\phi}_X A\right).$$

Note that $\bar{\phi}$ satisfies $\nabla^2\bar{\phi} = 0$, with the boundary conditions $\bar{\phi}_Z = \frac{2\omega k}{g}(|A|^2)_X$ on $z = 0$ and $\bar{\phi} \to 0$ as $z \to -\infty$. The free surface amplitude is obtained from $\eta = \frac{\epsilon\omega}{g}[(iA + \frac{\epsilon}{2k}A_x)e^{i\theta} - \frac{k^2\epsilon}{\omega}A^2e^{2i\theta}] + (*)$. We introduce the following dimensionless and translating variables: $T' = \omega T$, $X' = kX$, $Z' = kZ$, $\eta' = k\eta$, $\bar{\phi}' = \frac{2k^2}{\omega}\bar{\phi}$, $u = \frac{2\sqrt{2}k^2}{\omega}A$, $\tau = -\epsilon\frac{T'}{8}$, $\chi = X' - \frac{1}{2}T'$. Solving Laplaces equation on $-\infty \le Z \le 0$ by Fourier methods for $\bar{\phi}$ in terms of A yields the following perturbed nonlocal NLS equation (HONLS):

$$iu_\tau + u_{\chi\chi} + 2|u|^2u + \varepsilon\left(\frac{i}{2}u_{\chi\chi\chi} - 6i|u|^2u_\chi + iu^2u_\chi^* + 2u[H(|u|^2)_\chi]\right) = 0, \quad (3)$$

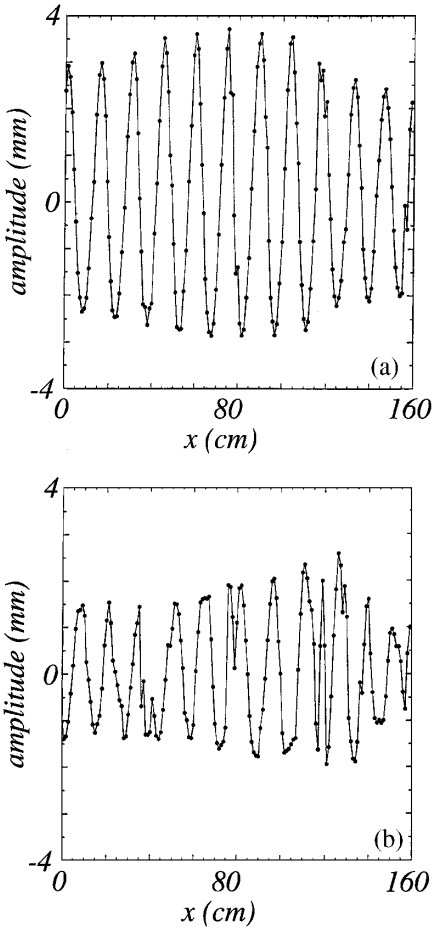

FIG. 2. Spatial envelope of the modulated wave train at (a) $t = 15$ sec and (b) $t = 40$ sec.

where $H(f)$ represents the Hilbert transform of the function f. The Fourier transform of the Hilbert transform yields $\widehat{H(f)} = i\,\mathrm{sgn}(k)\widehat{f(k)}$. These Fourier relations are readily implemented numerically. Note that Eq. (3) destroys even symmetry.

Solutions of the NLS equation [(3) for $\epsilon = 0$] with periodic boundary conditions can be described in terms of the Floquet spectrum of the following linear operator [4]:

$$\mathcal{L}(u;\lambda) = i\begin{pmatrix}1 & 0\\ 0 & -1\end{pmatrix}\frac{d}{dx} - \begin{pmatrix}0 & u\\ -u^* & 0\end{pmatrix} - \lambda I. \quad (4)$$

Using the fundamental solution matrix M, defined by the conditions $\mathcal{L}(u;\lambda)M = 0$ and $M(x,x;u,\lambda) = I$, we introduce the Floquet discriminant $\Delta(\lambda) = \mathrm{Tr}[M(x + L, x; u, \lambda)]$. The spectrum of $\mathcal{L}$ is given by the following condition on the discriminant: $\sigma(\mathcal{L}) = \{\lambda \in \mathbb{C} \,|\, \Delta(\lambda) \in \mathbb{R}, -2 \le \Delta(\lambda) \le 2\}$. The elements of the periodic spectrum that we monitor in the experiments are (a) simple points λ^s, specified by the condition $\Delta(\lambda)|_{\lambda=\lambda^s} = \pm 2$, $\Delta'|_{\lambda=\lambda^s} \neq 0$, and (b) double points λ^d, which satisfy the conditions $\Delta(\lambda)|_{\lambda=\lambda^d} = \pm 2$, $\Delta'|_{\lambda=\lambda^d} = 0$, $\Delta''|_{\lambda=\lambda^d} \neq 0$.

The spectrum is invariant under the NLS flow. Each periodic eigenvalue corresponds to a nonlinear mode whose structure and dynamical stability are determined by the location and order of the periodic eigenvalue. Complex double points are associated with linearized instabilities of the NLS equation [6,7,8,10]. The complex double points label the orbits homoclinic to unstable solutions and correspond to "sensitive" regions of phase space.

Consider the class of solutions related to perturbations of the periodic Stokes wave (for the NLS equation it is given by $u_0(t) = ae^{2ia^2t}$ where, for convenience, a is assumed to be real). After dimensionalizing and transforming to the surface displacement η, the exponent corresponds to the nonlinear frequency shift found by Stokes. Stability of the Stokes wave can be found by considering perturbations of the form $u(x,t) = u_0[1 + \epsilon(x,t)]$ and linearizing for small ϵ. Assuming $\epsilon(x,t) = \epsilon_n(0)e^{i\mu_n x + i\sigma_n t} + \epsilon_{-n}(0)e^{i\mu_{-n}x - i\sigma_{-n}t}$ and $\mu_n = 2\pi n/L$, the growth rate σ_n is given by $\sigma_n^2 = \mu_n^2(\mu_n^2 - 4a^2)$. Thus the solution is unstable provided that $0 < (\pi n/L)^2 < |a|^2$. This stability criterion is applicable to the modulated periodic wave train produced via $\eta_p(t)$ described in the laboratory experiments.

Numerical experiments.—We numerically study Eq. (3) and consider the following two classes of initial data:

(i) experimental data ("E") obtained near the wave maker (Fig. 2a); and (ii) theoretical data ("T") $u(x,0) = a(1 + \delta_T \cos\mu_n x)$. Reproducibility is studied by graphing η, the surface displacement evolution of $u(x,0)$ versus that of $u'(x,0) = u(x,0)[1 + \delta r(x)]$, where δ is on the level of experimental noise (1%–2%) [$r(x)$ is a random field]. All parameters in the numerical experiments have been carefully matched with the nondimensionalized parameters used in the laboratory experiments consistent with the assumption of deep water and omitting surface tension. We use a 4th order pseudospectral code for integrating HONLS with $N = 512$ Fourier modes in space and a 4th order adaptive Runge-Kutta scheme in time.

In [11] we have shown that for data T there are $2n + 1$ simple imaginary points in the spectrum: λ_0 and $\{\lambda_{n+}, \lambda_{n-}\}$, $n = 1, 2, \ldots, M$. When δ_T is asymptotically small, the distance of the simple points $\lambda_{n+}, \lambda_{n-}$ of the spectrum of $\mathcal{L}$ from a double point is $O(\delta_T^n)$, $n = 1, 2, \ldots, M$ and can be made arbitrarily small by taking M large enough. Since the effects of noise in the experiments are larger than the distance from the double points (for $M = 3$), perturbations of the eigenvalues due to noise are also important.

The results of the numerical study of (3) are consistent with the evidence of chaotic evolutions provided by the laboratory experiments. Using initial data E, for short times the experiment is reproducible and the phase plane plot stays close to the 45° line. As the wave field evolves, the experiment is rendered irreproducible. A nonremovable phase shift develops between the experiments that changes with time resulting in a phase plane plot that is strikingly similar to that of the laboratory data (Fig. 1d).

To investigate the chaotic evolution we use the associated nonlinear spectral theory of the NLS equation. The data provided by the physical and numerical experiments are projected onto the nonlinear spectrum of the NLS and we follow its evolution in time. The spectral results are striking. For data E there are initially seven simple nonreal eigenvalues which, as described above, are centered around three double points that correspond to three unstable modes. We found frequent and (apparently) persistent homoclinic transitions in all the excited modes, indicating a change in the nonlinear mode content and the characteristics of the modes. The wave train thus changes its features irregularly in space and time.

Although there is no mathematical proof of chaos, nevertheless on the physical time scales examined, the net result is serious temporal irregularities and apparently chaotic dynamics. We conclude two things: (i) the HONLS equation causes significant temporal movement of the spectrum and numerous homoclinic transitions. In this parameter regime, the NLS is not an adequate approximation to the water wave problem. (ii) Remarkably, the chaotic dynamics observed for HONLS bears many similarities to the chaotic dynamics observed in other perturbed NLS equations, most notably the discrete systems with noneven initial data studied in Ref. [8], only here the eigenvalues evolve significantly away from the imaginary axis. Further, we do not observe homoclinic crossings as in [6,7].

The other periodic wave trains we studied using HONLS corresponded to model data T. We considered cases for $M = 1, 3, 5$ nearby unstable modes, all with $\delta_T = 0.1$. For $M = 1$ we found that the phase plane diagnostic produces the 45° line. The end points of the spectrum remained well separated by large "gaps" during the experiment and did not evolve into sensitive regions; regular nonchaotic dynamics ensued. For this case the NLS equation gives an adequate description of the dynamics.

The situation for $M = 3$ was found to be qualitatively similar to the experimental data (as expected). For the case $M = 5$ we found that the phase plane plot diverges from the 45° line even more strongly than for $M = 3$. The spectrum evolved significantly and we found more numerous homoclinic transitions than with $M = 3$. The cases $M = 3, 5$ yield strong temporal irregularities and, for the time scales under consideration, chaotic dynamics.

Finally we mention a "theoretical" soliton case using HONLS for initial data $u(x,0) = a\,\mathrm{sech}(ax)$. The phase plane plot remains close to the 45° line with little spread (Fig. 1c), as was observed in the laboratory. The spectral plots indicate widely separated simple eigenvalues which do not evolve near sensitive regions. The soliton case was found to be reproducible and reflects a stable nonchaotic evolution which NLS adequately describes.

This work was partially supported by the AFOSR USAF, Grant No. F49620-97-1-0017 and the NSF Grants No. DMS-9703850, No. DMS-9803567, and No. DMS-9972210.

[1] G. G. Stokes, Camb. Trans. **8**, 441–473 (1847).
[2] T. Levi-Civita, Math. Ann. **xciii**, 264 (1925).
[3] T. B. Benjamin and J. E. Feir, J. Fluid Mech. **27**, 417–430 (1967).
[4] M. J. Ablowitz and H. Segur, *Solitons and the Inverse Scattering Transform* (SIAM, Philadelphia, 1981).
[5] H. C. Yuen and B. M. Lake, Phys. Fluids **18**, 956–960 (1975).
[6] M. J. Ablowitz, C. Schober, and B. M. Herbst, Phys. Rev. Lett. **71**, 2683–2686 (1993).
[7] D. W. McLauughlin and C. M. Schober, Physica (Amsterdam) **57D**, 447–465 (1992).
[8] M. J. Ablowitz, B. M. Herbst, and C. M. Schober, Physica (Amsterdam) **228A**, 212–235 (1996).
[9] K. B. Dysthe, Proc. R. Soc. London A **369**, 105–114 (1979).
[10] N. Ercolani, M. G. Forest, and D. W. McLaughlin, Physica (Amsterdam) **43D**, 349–384 (1990).
[11] M. J. Ablowitz and C. M. Schober, Contemp. Math. **172**, 253–268 (1994).